Hindawi
Advances in Materials Science and Engineering
Volume 2022, Article ID 4021618, 19 pages
https://doi.org/10.1155/2022/4021618

Research Article

The Influence of Nano Titanium as Bitumen Modifier in Stone Mastic Asphalt

Khairil Azman Masri[1,2] **Nur Syafiqah Shamimi Mohd Zali**[1] **Ramadhansyah Putra Jaya**[1] **Mazlan Abu Seman**[1] **and Mohd Rosli Mohd Hasan**[3]

[1]*Department of Civil Engineering, College of Engineering, Universiti Malaysia Pahang, 26300 Gambang, Kuantan, Pahang, Malaysia*
[2]*Earth Resources and Sustainability Centre (ERAS), Universiti Malaysia Pahang, 26300 Gambang, Kuantan, Pahang, Malaysia*
[3]*School of Civil Engineering, Universiti Sains Malaysia, Engineering Campus, 14300 Nibong Tebal, Pulau Pinang, Malaysia*

Correspondence should be addressed to Khairil Azman Masri; khairilazman@ump.edu.my

Received 10 November 2021; Revised 7 January 2022; Accepted 4 March 2022; Published 11 April 2022

Academic Editor: Qian Chen

Nanomaterials are emerging as one of the methods to improve the pavement industry. Due to that, this study explores the influence of nano TiO_2 modified binder and mixture with 60/70 grade bitumen. The first stage discovers the physical properties of bitumen by undergoing penetration and softening point tests. Then, the nano TiO_2 modified binder is evaluated in terms of its morphological and chemical properties. To verify the modified binder design, the mechanical performance of stone mastic asphalt (SMA) is assessed in terms of volumetric properties. From the results, 5% nano TiO_2 modified binder shows significant improvement in terms of penetration and softening point. The results also show that the 3% nano TiO_2 modified binder contributes the highest improvement in terms of its chemical properties and the morphological properties. Based on the morphological properties' evaluation, FTIR and XRD observed a sharp peak of nano TiO_2 while the bitumen containing nano TiO_2 is well distributed when SEM-EDX was applied. In addition, the volumetric properties of SMA also significantly improve with the addition of nano TiO_2. It can be said that the addition of nano TiO_2 is able to enhance the overall properties of bitumen.

1. Introduction

Stone mastic asphalt has widely been used in countries such as Unites States, Europe, and Asian countries like Malaysia [1]. The need to use SMA is due to the increasing traffic users over the years which make SMA a suitable choice since it is known to withstand high loads [2]. SMA originated from Germany only consists of coarse aggregates and bitumen as a filler in which the mix is held by the strong elastic properties of the binder [3]. However, with modernisation and new technology introductions, the SMA has been incorporated with many materials in such ways that the materials can improve the SMA properties. A modification to the mixture is one of the methods introduced. Some suggested changes include adding materials as an additive, rejuvenators, or even stabilizers. The focus would be on the aftereffect of the mechanical effect that the materials have on the SMA, but binder modification has not been further researched in depth [4].

Nanomaterials are chemical compounds or products that are processed and used on a very small scale. The size of nanomaterials is between 1 to 100 nanometres (nm) [5]. They previously have been used in the healthcare industry, beauty products, and biology-related field, and it is priorly used in construction also before embarking to the pavement industry [6]. Nanomaterials have many types of applications depending on their respective type and size. Some of the commonly used nano materials that are always encountered are nano clay, nano silica, nano-sized metals such as copper, zinc, and aluminium oxide [7]. Aging is a concern of asphalt mixtures, and there are two types of it which are thermal oxidative aging and photo oxidative aging [8]. This is where

the surface modified nanomaterials such as nano silica, nano zinc oxide, and nano TiO_2 act as they could improve the antiaging behaviour of asphalt [9].

Nano clay is naturally occurring minerals, and its purity could affect the final nanocomposite properties. Due to their low cost of production, it is commonly used as it has potential to improve mechanical and thermal binder properties [10]. Nano silica properties such as its good stability, affordable cost, high surface area, chemical purity, and good dispersing ability have made it one of the most used materials over the years in improving the mechanical performance of asphalt such as aging, fatigue, and cracking [11].

Among the mentioned nanomaterials, nano TiO_2 was chosen due to its properties such as higher reactivity with bitumen due to its small size [12]. It possesses photocatalytic properties which could help in eliminating hazardous gases like nitrogen monoxide [13]. This promotes the environmentally friendly area of the asphalt pavement. Nano TiO_2 also improve the asphalt aging properties [14]. Furthermore, nano TiO_2 could reduce binder drain down properties by increasing the adhesion between aggregates and bitumen when added into the mix as the nano particles fill the voids that is present and make the structure more compact [15].

This study is aimed to investigate the binder modification by incorporating it with nano titanium and its effect to the SMA. Different percentages of nano TiO_2 starting from 1 to 5% will be mixed with the bitumen and will further be accessed. Among the test that will be done on the samples would be the traditional bitumen test which are penetration test and softening point. Then, the sample would be further analysed in terms of morphology and chemical aspects by Fourier transform method analysis (FTIR), scanning electron microscope (SEM-EDX), and X-ray diffraction analysis (XRD). The volumetric properties of SMA are also investigated after the nano TiO_2 modified bitumen is included in the SMA mix. The test results show that 3% nano TiO_2 modified bitumen has improved the bitumen in terms of its physical properties, rheology, morphology, and chemical characteristics. The volumetric properties of SMA also experience positive enhancement due to the binder modification.

2. Materials and Methods

2.1. Nano Titanium. The sizes of nano TiO_2 are between 10 to 15 nanometres and in white powder form supplied by the local supplier. Table 1 shows the properties of nano TiO_2 used for experimental works. Based on Table 1, the usage of nano TiO_2 is suitable for bitumen modification due to its high melting and boiling point as well as its structure.

2.2. Bitumen. The bitumen currently utilised has a 60/70 penetration grade. Table 2 shows the properties of the asphalt binder used in the experimental works.

2.2.1. Preparation of Nano TiO_2 Modified Binder. A mechanical mixer was used to prepare the nano TiO_2 modified binder at 1500 rpm and 160°C for 60 minutes. A predetermined amount of bitumen was obtained and put in the oven for approximately 1.5 to 2 hours until it melted. About 500 g of bitumen was then weighted before mixing with 1 to 5% nano TiO_2. The mixture was mixed for 30 minutes while adding the nano TiO_2 gradually and further 30 minutes of additional mixing to ensure its homogeneity.

Table 1: Properties of nano TiO_2.

Properties	Descriptions
Colour	White
Purity	99.9%
Primary particle size	20 nm
Structure	Anatase, Rutile, Brookite
Melting point	1843°C
Boiling point	2972°C
Relative density at 25°C	4.26 g/cm3

2.3. Experimental Methods

2.3.1. Stone Mastic Asphalt (SMA) Sample Preparation. SMA samples were prepared according to the Malaysian standard specification JKR/SPJ/S4, by incorporating 6.16% optimum binder content [16] and compacted using a Marshall compactor with 50 blows on each face. Figure 1 represents the aggregate grading used to fabricate asphalt mixture specimens. Sieve analysis was performed to obtain the required aggregated mass based on the targeted specification. The SMA aggregate grading is shown in Figure 1.

2.3.2. Morphological Tests for the Bitumen

(1) Fourier Transform Infrared (FTIR) Spectroscopy. Fourier Transform infrared (FTIR) spectroscopy is an analytical technique used to identify organic, polymeric, and, in some cases, inorganic materials. The technique uses infrared light to scan test samples and observe chemical properties. The qualitative analysis identifies characteristic absorption peaks for the functional group of interest, such as polymer components, carbon, and sulphur oxidation products [17]. In this study, the attenuated total reflectance Fourier-transform infrared (ATR-FTIR) spectroscopy was used to evaluate the modified binder. The sample was prepared by cooling off the bitumen-nano TiO_2 mixture before being compacted into a small sphere and placed on a small microscopic slide.

(2) X-Ray Diffraction (XRD). X-ray diffraction or XRD is a nondestructive test method used to analyse the structure of crystalline materials. XRD analysis identifies crystalline phases present in a material, revealing chemical composition information. X-rays are directed toward samples by applying the voltage, and reflected X-rays are gathered by the detector [18]. The phase identification of bitumen was analysed using XRD at [°2θ] theta. Samples were prepared by cooling the bitumen mixture and made into small solid spheres. XRD graph peaks were produced after the testing was finished.

Table 2: Properties of 60/70 grade bitumen.

Properties	Descriptions	Material used
Specific gravity @25°C	1.01/1.06 kg/cm^3	1.03
Penetration @25°C	60–70 mm	65
Softening point @25°C	49–56°C	53
Ductility @25°C	100 cm	100

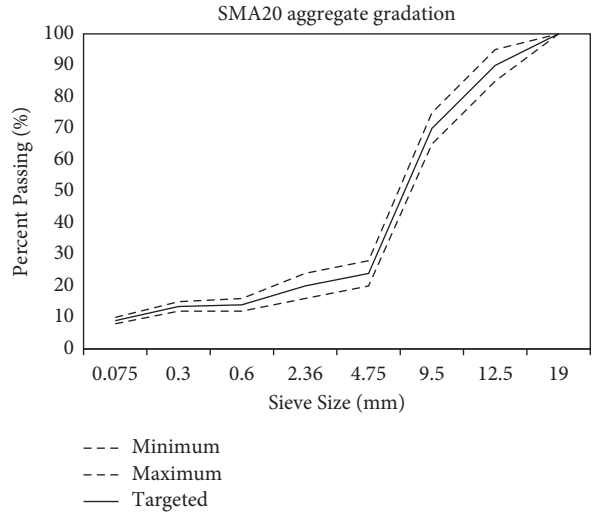

Figure 1: The SMA aggregate grading.

2.3.3. Scanning Electron Microscopy with Energy Dispersive X-ray Analysis (SEM-EDX). Scanning electron microscopy (SEM) with energy dispersive X-ray analysis (EDX) provides detailed high-resolution images of the sample by reprojecting a focused electron beam across the surface and detecting secondary or backscattered electron signal. Sample preparation involves cooling the bitumen until it hardens before scrapped into a small portion and observed under the microscope at desired magnifications. Further analysis using EDX was performed to identify the elements present in bitumen samples.

2.3.4. Physical Tests for Bitumen

(1) Softening Point. Bitumen was melted and poured into a pair of rings placed on a plate covered with Vaseline. After the specimen cooled, the ring was suspended in distilled water at 5 ± 2°C for 15 minutes. Steel balls were also placed on the surface of the bitumen in the ring. Then, the bath liquid was stirred and heated at a rate of 5 ± 2°C per minute. A thermometer was placed in the middle of the ring holder, levelled with the bottom of the ring. When the ball passed and dropped into the base plate, the temperature was recorded.

(2) Penetration Test. Specimens were prepared in a sample container and placed in a water bath at room temperature for 1 to 1.5 hours before the test. Then, the penetrometer dial reading was set to zero. The penetration needle was cleaned and fixed into the holder and guide. For a normal test, the precisely dimensioned needle was loaded to 100 ± 0.05 g. Next, the needle was slowly lowered until the tip makes contact with its image on the sample's surface at right angles. The needle holder was released to penetrate the bitumen for 5 ± 0.1s at a constant temperature of 25 ± 0.1°C. The penetration was measured in millimetre (mm).

2.3.5. Volumetric Properties of SMA. This test was conducted on eight samples with two samples each for 0%, 2%, 3%, and 4%. Before testing, the samples were conditioned by placing them in a water bath at a temperature of 60°C for 30 minutes. Then, the samples were placed on a Marshall stability machine and subjected to a force sufficient to break the sample to determine the Marshall Stability. Volumetric properties obtained such as density, stability, flow, and stiffness were recorded.

The following tests were conducted according to the flowchart provided Figure 2.

3. Results and Discussion

3.1. Fourier Transform Infrared Spectroscopy. Figure 3(a) shows the IR spectrum of the original bitumen experiencing a N-H stretching at 3395.75 cm^{-1}. This peak is observed at the 3100–3500 cm^{-1} region which it could be seen that it appears as a wide and broad-shaped spectrum with medium strength. The spectrum then becomes longer and shorter as more nano TiO_2 is added. The two peaks at 2923.75 cm^{-1} and 2852.09 cm^{-1} which later appears are related to the C-H symmetric stretching (-CH2) and the C-H asymmetric vibrations (-CH3 and -CH2) due to the presence of hydrocarbon chain segments that usually exist in the bitumen. Figure 3(b) shows some of the functional groups for the bitumen.

Next, from Figure 3(c), it shows that all of the nano TiO_2 modified bitumen have almost the same peaks, but at 3% nano TiO_2 modified bitumen, there is a new absorption bond that is observed. That is when nano TiO_2 is included the original region of 3100–3500 cm^{-1} which then makes the N-H bonds does not appear anymore. It is instead replaced with the two peaks at the 2851–3100 cm^{-1} region which are 2923.14 cm^{-1} and 2851.96 cm^{-1}. These peaks appear as there are interactions between the C-H and O-H bonds of the nano titanium with the bitumen mix; these bonds are stretching with medium strength. The results are consistent with a study by Lin et al.

Going into the 1700 cm^{-1} region, a remarkable peak at 1700.49 cm^{-1} is observed at the carboxylic region indicating that oxidation happens in this region and carbonyl group (C = O) is present. Next, the two peaks observed at 1462.37 cm^{-1} and 1376.67 cm^{-1} are assigned to the O-H bond which experiences bending with medium strength. In which this 1376.67 cm^{-1} peak is a response to the phenol group. Lastly, the 721.20 cm^{-1} peak is due to the presence of C double bond (C = C) in the nano TiO_2 modified bitumen sample.

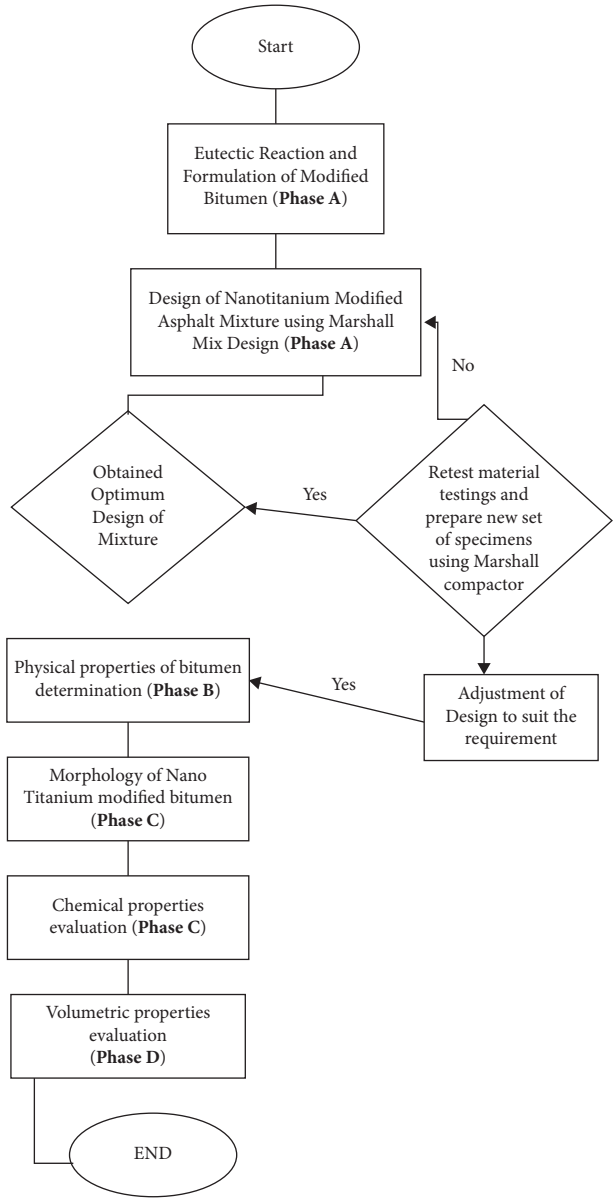

Figure 2: Flowchart of the research approach.

3.2. X-Ray Diffraction (XRD). Figures 4 and 5 depict the result of XRD on the unmodified and modified bitumen with nano TiO_2 sample. A close check on the nano TiO_2 powder is also done revealing that the nano titanium is of crystallised structure since sharp peaks are produced along the 25–75-degree peaks. The peak for the virgin bitumen is observed between 20–25 degree which has the peak 23.96 and 26.27 degrees as these peaks are due to the aliphatic chains and layers of condensed saturated rings since it is plain bitumen and is completely amorphous.

After the addition of nano TiO_2 in the bitumen, all of the samples show that the peak intensity rises, and this indicates that the nano TiO_2 particles have successfully incorporated themselves into the bitumen since the starting peak is higher than the starting peak for the original bitumen. The result trend is consistent with a study by Razavi and Kavussi [18]. The highest starts from 2%, followed by 3%, 5%, 4%, and 1%. But only 2% and 3% show that the peak intensity continues to develop up until 60 and 63 degrees, respectively. 3% is chosen as the bitumen continues to develop furthest with the influence of nano TiO_2. This shows that a little amount of nano TiO_2 such as 2% is able to contribute to the inner structure improvement of virgin bitumen.

3.3. Scanning Electron Microscopy with Energy Dispersive X-Ray Analysis (SEM-EDX). Figure 6 shows the morphology of the bitumen both before and after being added with nano titanium powder. Again, SEM analysis is performed to see the condition of the nano titanium when mixed with bitumen. For the unmodified bitumen, the black stripe is the bitumen in the liquid state, and since the sample is semisolid,

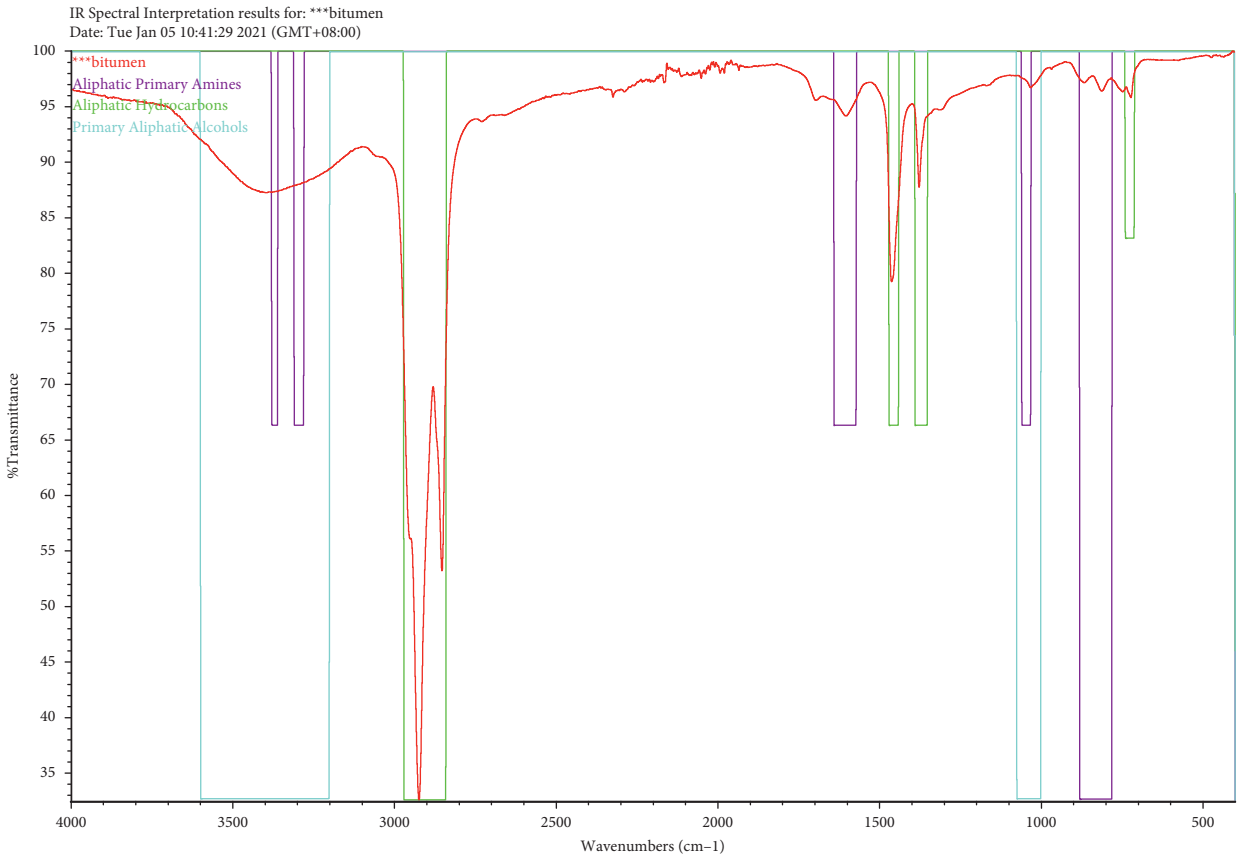

(a)

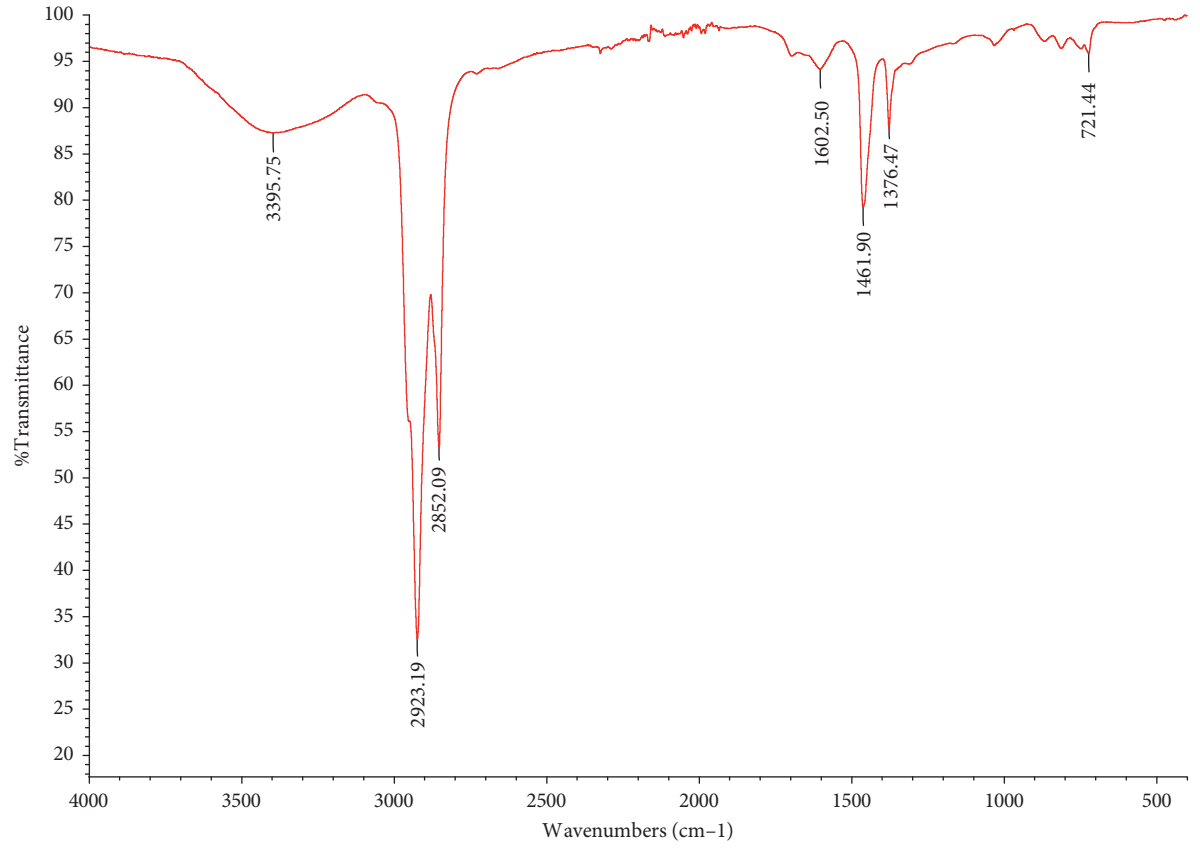

(b)

Figure 3: Continued.

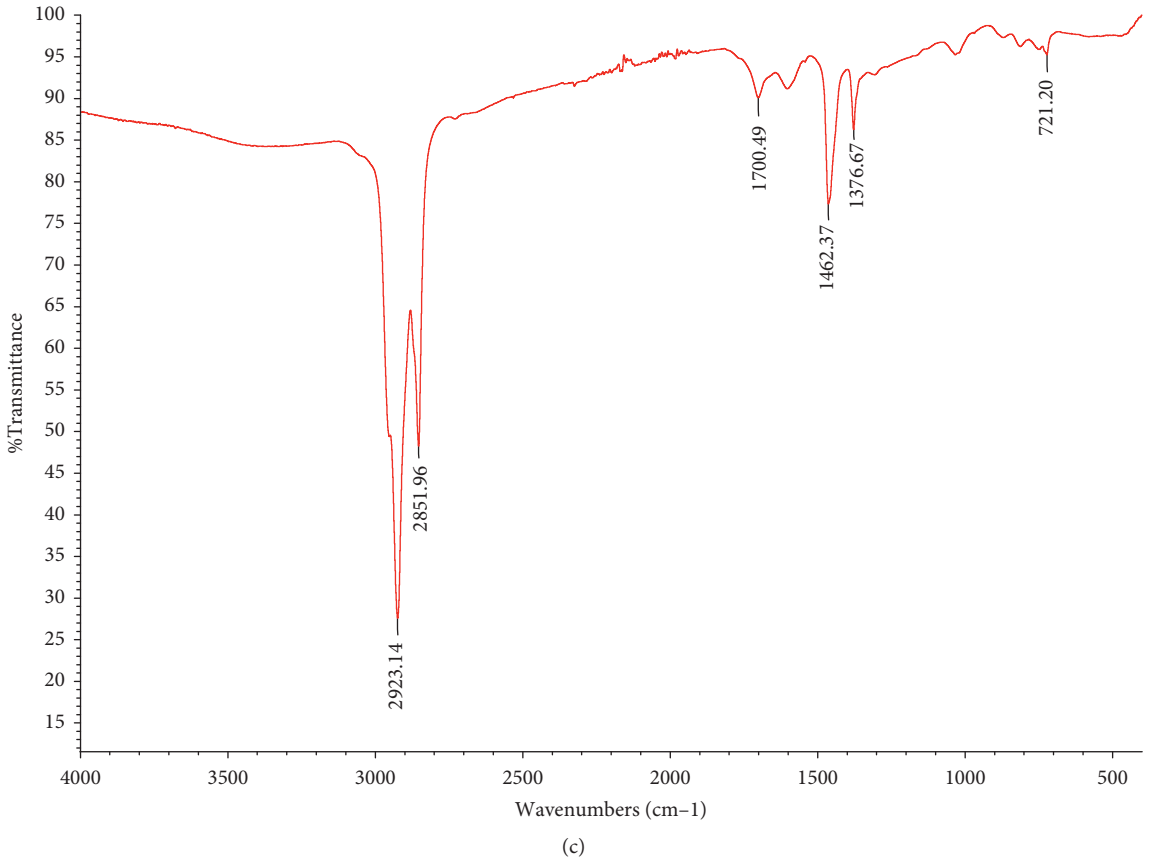

Figure 3: (a) Transmittance peaks of unmodified bitumen. (b) Transmittance (%) vs. wavenumber (cm^{-1}) spectral interpretation of unmodified bitumen. (c) Transmittance peaks of 3% nano TiO_2 modified bitumen.

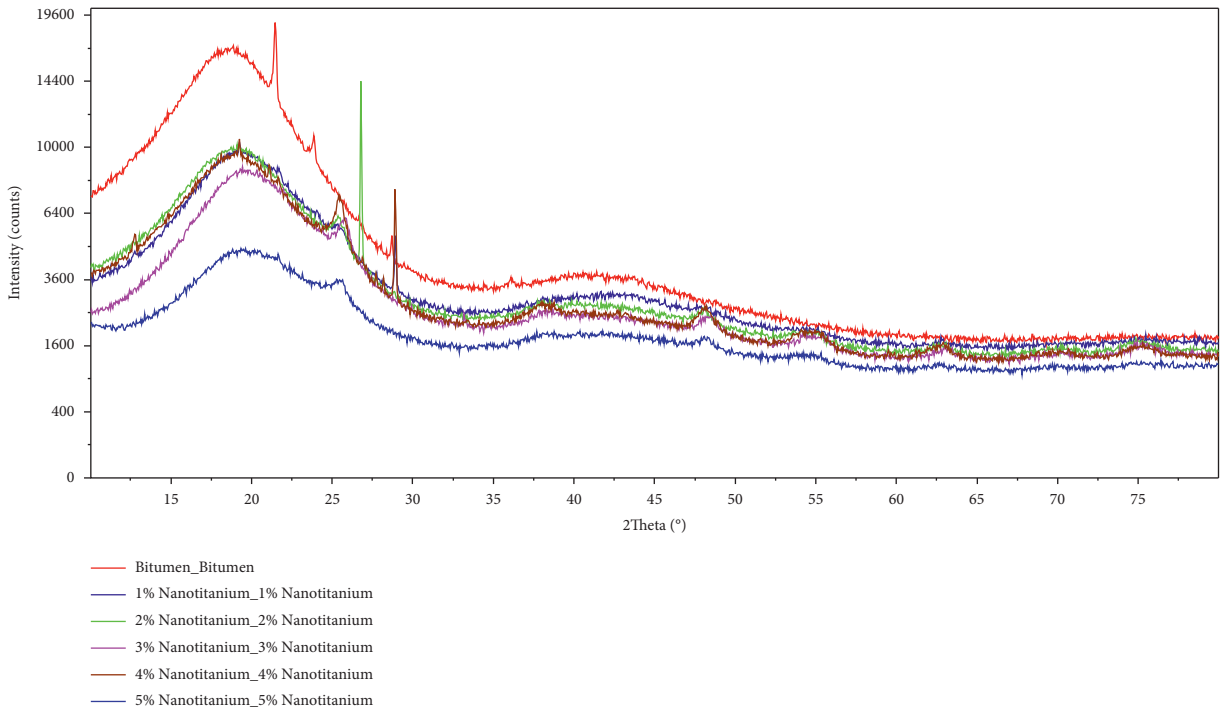

Figure 4: XRD for nano TiO_2 modified binder.

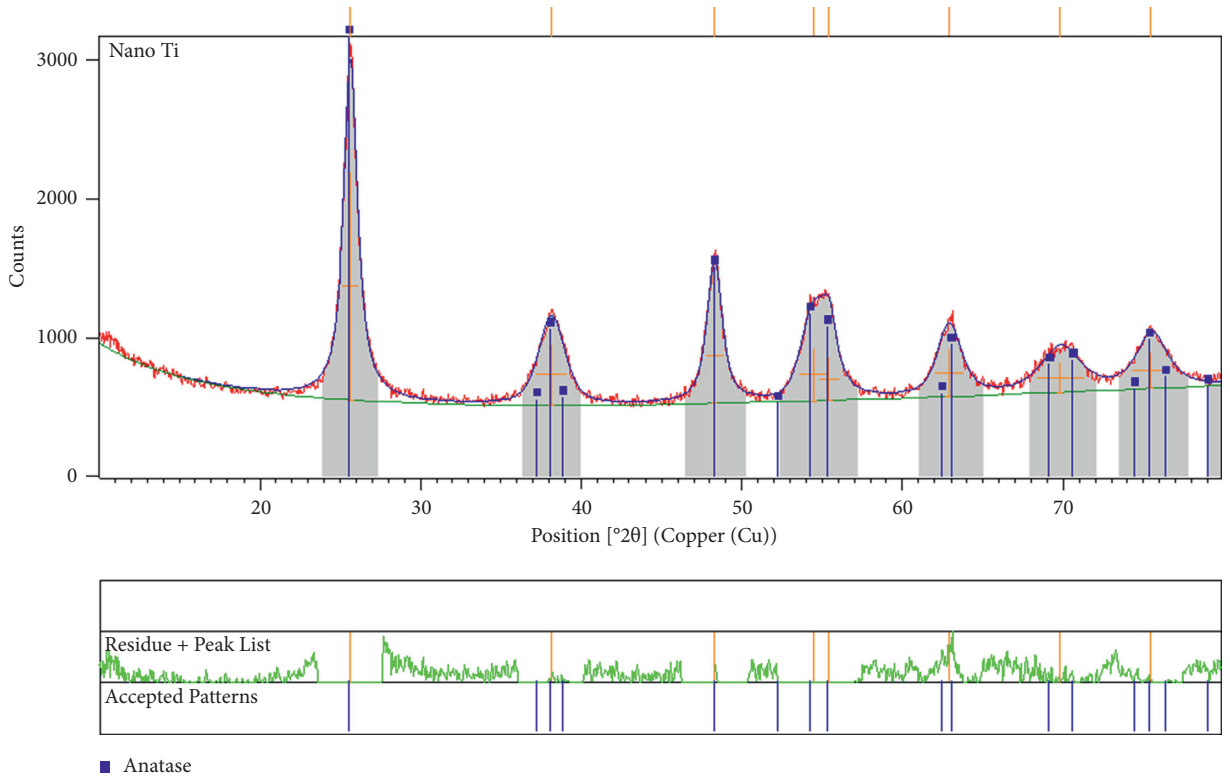

Figure 5: XRD peaks of Nano TiO_2 powder.

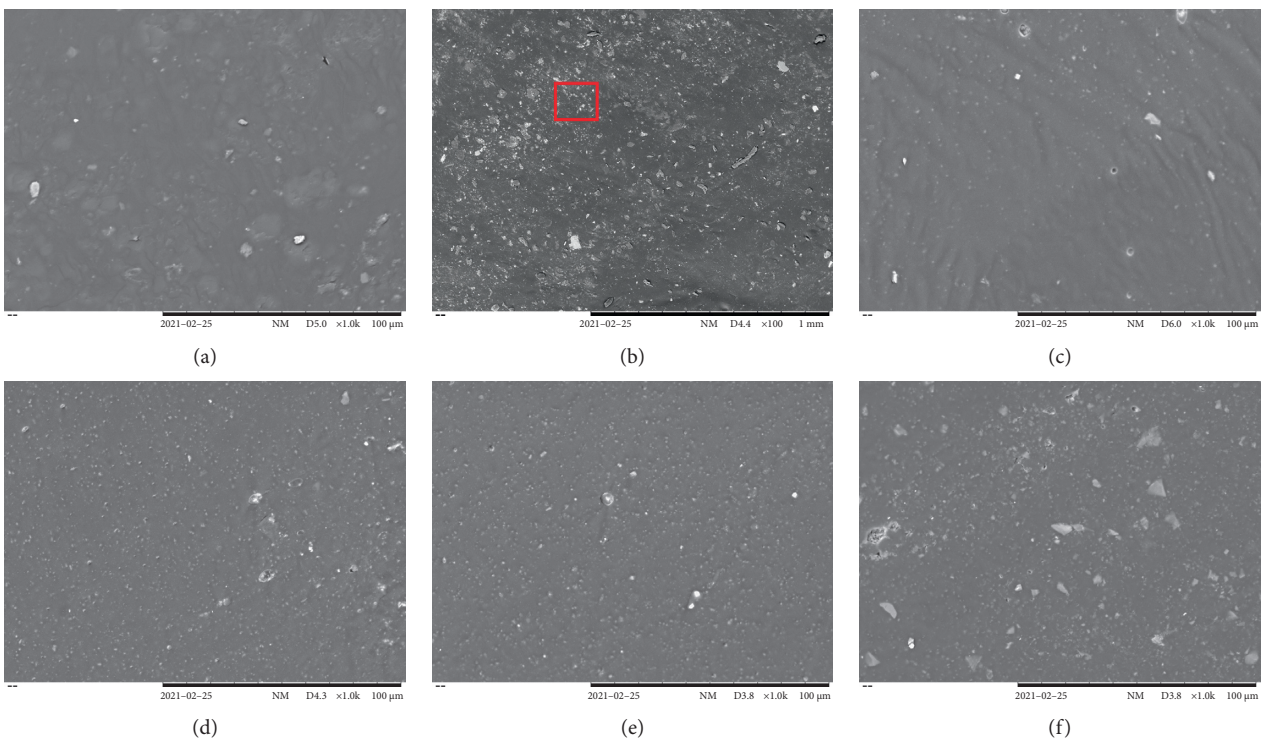

Figure 6: SEM images of modified and unmodified bitumen samples.

Table 3: Unmodified and modified bitumen elements.

Nano titanium (%)	Carbon		Oxygen		Sulphur		Titanium	
	Weight (%)	Atomic (%)	Weight (%)	Atomic (%)	Weight (%)	Atomic (%)	Weight (%)	Atomic (%)
0	76.36	84.83	12.32	10.28	5.68	2.36		
1	96.49	98.69	—	—	3.25	1.24	0.26	0.07
2	91.70	96.94			6.56	2.60	1.75	0.46
3	96.11	98.99			3.50	1.50	3.89	1.00
4	86.06	91.5	8.00	6.39	3.62	1.44	3.88	1.05
5	84.94	91.88	6.22	5.05	4.96	2.01	3.88	1.05

there seems to be a melted bitumen state and dry bitumen from the image.

The images generated from Figure 6 show the 0%, 1%, 2%,3%, 4%, and 5% addition of nano TiO_2. The images generated show that some nano TiO_2 powder is still not blended well into the bitumen and the white spots are the powders that has not been able to mix with the bitumen. This can be further verified with reference to the previous Table 1 (properties of nano TiO_2). With the increasing amount of nano TiO_2, the bitumen has difficulty in blending well with the nano TiO_2 which then produces insoluble white lumps that is observed with increasing nano TiO_2 powder. Meanwhile, 3% nano TiO_2 modified bitumen can mix thoroughly and have lesser white streaks or clumps. However, the dispersion is still acceptable, and the improvement is verified based on the obtained results.

Next, EDX analysis is also carried out on the samples; from the elements observed from Table 3 and Figures 7(a)–7(f), it is most likely that the white flakes or clumps observed are from the aluminium or calcium residue composed in the bitumen. The visibility is due to the amount of those elements that still exists inside the nano TiO_2 modified sample. The elements from table confirm that the most abundant elements are carbon and oxygen. Other elements that are obtained include aluminium, sulphur, and calcium. The results are consistent with a few recent studies performed by Snehal et al. [11], Arshad et al. [19], and Babagoli [15].

The unmodified bitumen shows all the elements mentioned before, but when nano TiO_2 is added with various content, the chemical composition changes according to the amount of nano TiO_2 added. Hence, the optimum nano TiO_2 content in terms of SEM-EDX analysis is at 3% nano TiO_2 modified bitumen followed by 5%, 4%, 2%, and 1%, as shown in Table 3. Only two elements are present: carbon and oxygen, which mainly made up the sample alongside nano TiO_2 showing that the nano TiO_2 is mostly blended with the bitumen. Overall, 3% specimen has the most influence on the chemical composition changes and enhancement of virgin bitumen.

3.4. Softening Point. As shown in Figure 8, the softening point is the highest at 0% nano TiO_2 at 44.4°C compared to 5% nano TiO_2 which only record at 41.8°C. Further addition of nano TiO_2 makes the softening points drop lower than the initial reading recorded. The high softening point at 0% implies that the resistance of the bitumen to the heat is increased and shows that there is a low probability that the bitumen will soften under high temperatures which is a resemblance of the hot weather. However, 4°C is not a large difference, and usually in summer seasons, the temperature on pavement surface is larger than 50°C, so with this bitumen, the risk of rutting exists always. This makes the bitumen less vulnerable when temperature changes. Rutting is one of the deformations happening related to temperature, and with this increase in softening point, the rutting would be reduced. The readings recorded are having the same trend as previous research by Crucho et al. [20] in which the increasing content of nano material added results in lower softening point.

3.5. Penetration Test. The results in Figure 9 show that bitumen penetration varies with different nano TiO_2 percentages. The penetration for nano TiO_2 mixture between 1 to 5% are 73 dmm, 61.5 dmm, 60.5 dmm, 55.5 dmm, 54.5 dmm, and 54 dmm, respectively. The consistency of bitumen is harder at 3% to 5% nano TiO_2 compared with 0% nano TiO_2 sample. This result is consistent with the earlier study on nano silica that observed a decrease in penetration tests [20]. These results are also reflected in the nano TiO_2 usage in the binder, which is similar to the utilisation of nanomaterials. This is caused by the increased viscosity of bitumen, as evident from the penetration value at increasing nano titanium percentages. Essentially, nano TiO_2 addition caused bitumen to be more consistent and harder. Thus, improving rutting resistance produces much stiffer bitumen which affects the resistance to fatigue cracking.

3.6. Volumetric Properties

3.6.1. Stability. Figure 10 shows the density and stability of the modified binder against nano TiO_2 percentages between 0 to 4%. The stability of the mixture is mostly influenced by the cohesion and internal friction of the matrix, which supports the coarse aggregates [21]. Figure 10 shows a comparable trend for density and stability, especially for the 3% nano TiO_2 addition. For this particular sample, the density is 2.238 g/cm^3, while the maximum stability is 5945 N compared to 5879 N for 0% nano TiO_2 addition. It is found that increasing nano TiO_2 amount also increases the stability and density. However, nano TiO_2 addition beyond 3% does not increase both parameters. This indicates that the usage of 3% nano TiO_2 in SMA mixture is more effective in enhancing density and stability. These contribute to less

Spectrum details

Project:	New project	Spectrum name:	Spectrum 1

Electron Image

Image Width: 351.4 μm

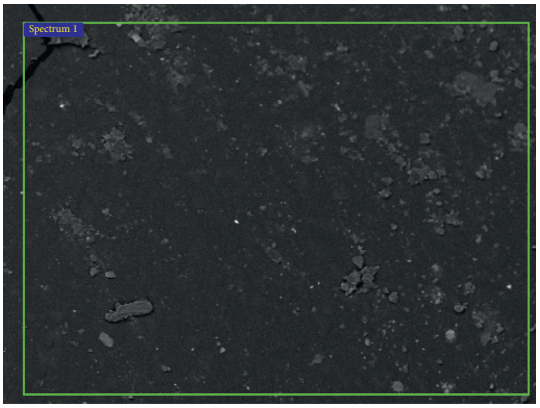

Acquisition conditions

Acquisition time (s) :	30.0	Process time :	5
Accelerating voltage (kV) :	15.0		

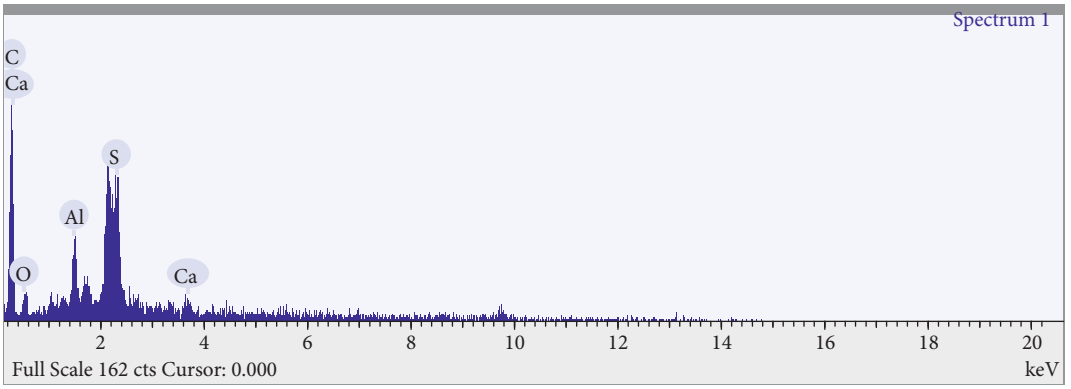

Quantification Settings

Quantification method :	All elements (normalised)	Coating element :	None

Summary results

Element	Weight %	Weight % σ	Atomic %
Carbon	76.361	3.052	84.832
Oxygen	12.322	3.166	10.277
Aluminum	4.031	0.526	1.993
Sulfur	5.677	0.962	2.363
Calcium	1.608	0.580	0.535

(a)

Figure 7: Continued.

Spectrum details

Project:	New project	Spectrum name:	Spectrum 1

Electron Image

Image Width: 175.7 μm

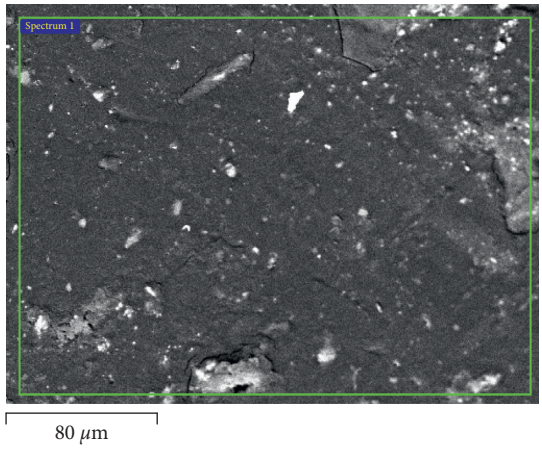

Acquisition conditions

Acquisition time (s) :	29.9	Process time :	5
Accelerating voltage (kV) :	15.0		

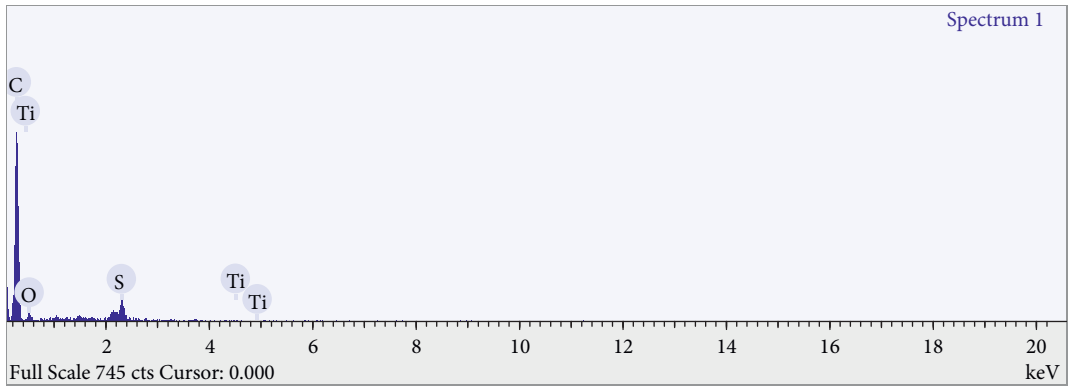

Quantification Settings

Quantification method :	All elements (normalised)	Coating element :	None

Summary results

Element	Weight %	Weight % σ	Atomic %
Carbon	96.490	0.469	98.689
Oxygen	0.000	0.000	0.000
Sulfur	3.246	0.395	1.244
Titanium	0.264	0.261	0.068

(b)

Figure 7: Continued.

Spectrum details

Project:	New project	Spectrum name:	Spectrum 1

Electron Image

Image Width: 351.4 μm

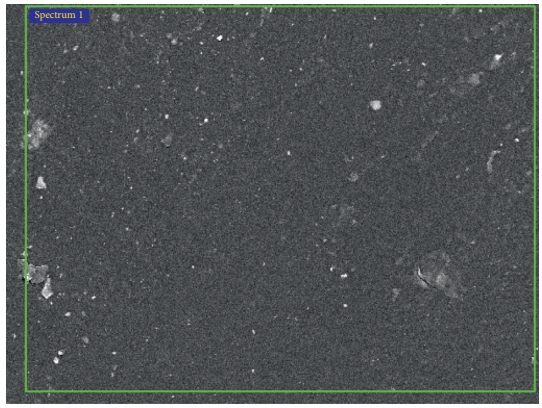

Acquisition conditions

Acquisition time (s) :	29.9	Process time :	5
Accelerating voltage (kV) :	15.0		

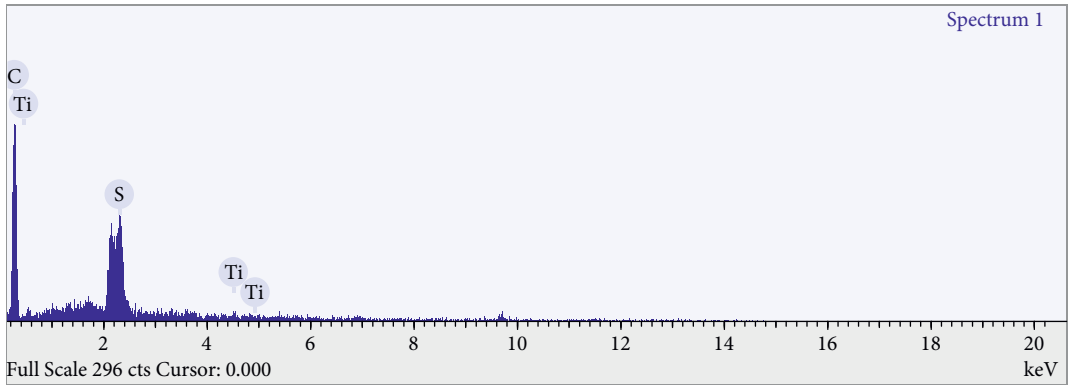

Quantification Settings

Quantification method :	All elements (normalised)	Coating element :	None

Summary results

Element	Weight %	Weight % σ	Atomic %
Carbon	91.695	1.105	96.940
Sulfur	6.559	0.914	2.598
Titanium	1.745	0.656	0.463

(c)

Figure 7: Continued.

Spectrum details

Project:	New project	Spectrum name:	Spectrum 1

Electron Image

Image Width: 351.4 μm

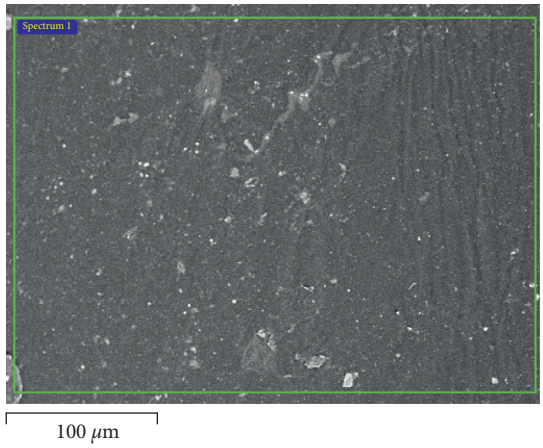

Acquisition conditions

Acquisition time (s) :	30.0	Process time :	5
Accelerating voltage (kV) :	15.0		

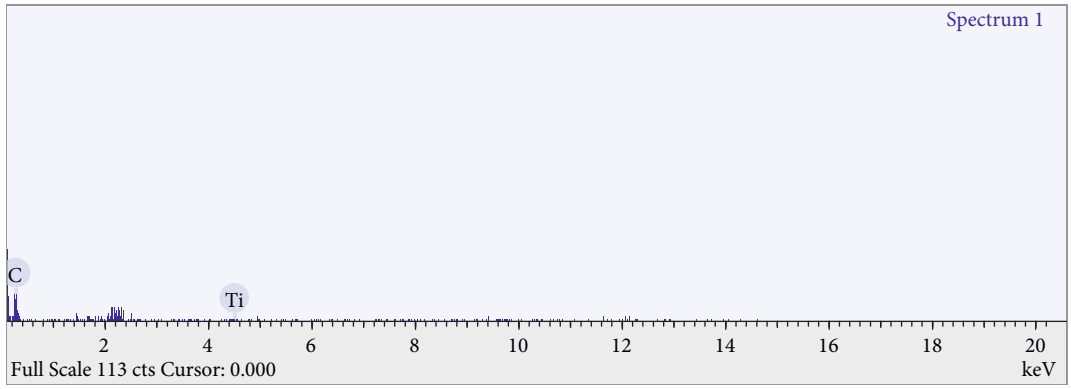

Quantification Settings

Quantification method :	All elements (normalised)	Coating element :	None

Summary results

Element	Weight %	Weight % σ	Atomic %
Carbon	96.107	4.005	98.994
Titanium	3.893	4.005	1.006

(d)

Figure 7: Continued.

Spectrum details

Project:	New project	Spectrum name:	Spectrum 1

Electron Image

Image Width: 351.4 μm

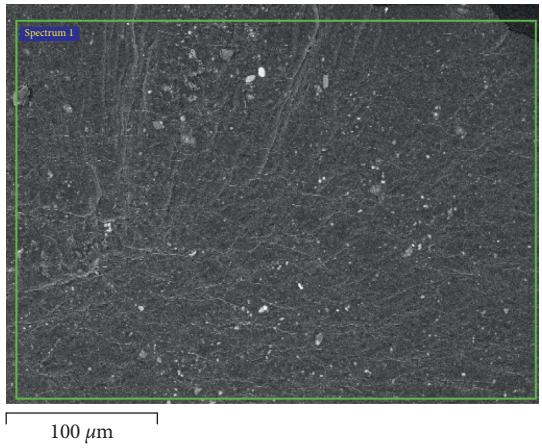

Acquisition conditions

Acquisition time (s) :	30.0	Process time :	5
Accelerating voltage (kV) :	15.0		

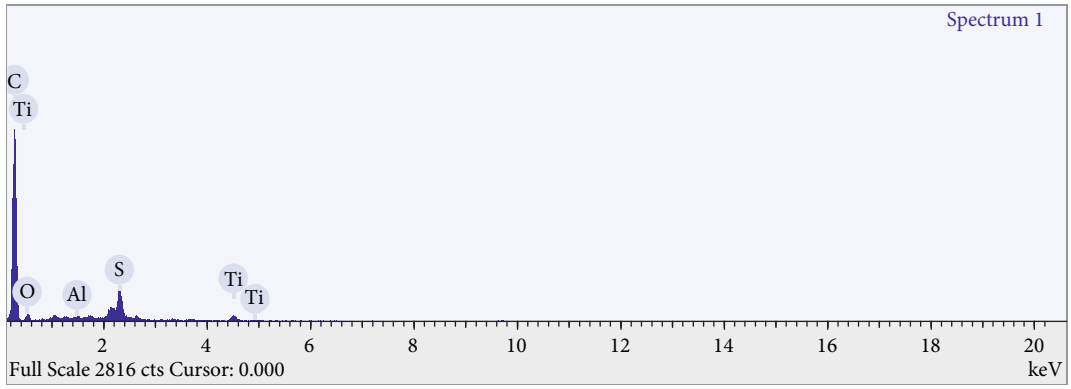

Quantification Settings

Quantification method :	All elements (normalised)	Coating element :	None

Summary results

Element	Weight %	Weight % σ	Atomic %
Carbon	86.055	1.011	91.499
Oxygen	8.001	1.039	6.387
Aluminum	0.250	0.073	0.118
Sulfur	3.624	0.192	1.444
Titanium	2.070	0.183	0.552

(e)

Figure 7: Continued.

Spectrum details

Project: New project Spectrum name: Spectrum 1

Electron Image

Image Width: 351.4 μm

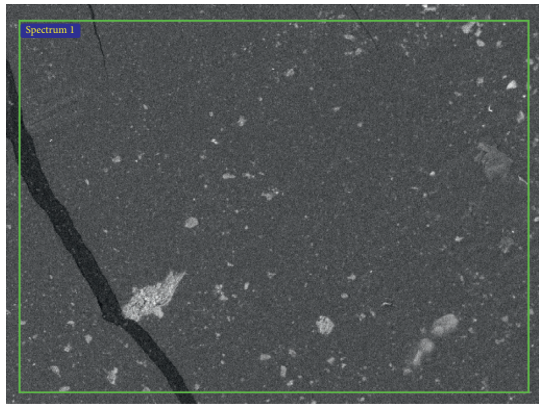

Acquisition conditions

Acquisition time (s) : 29.9 Process time : 5

Accelerating voltage (kV) : 15.0

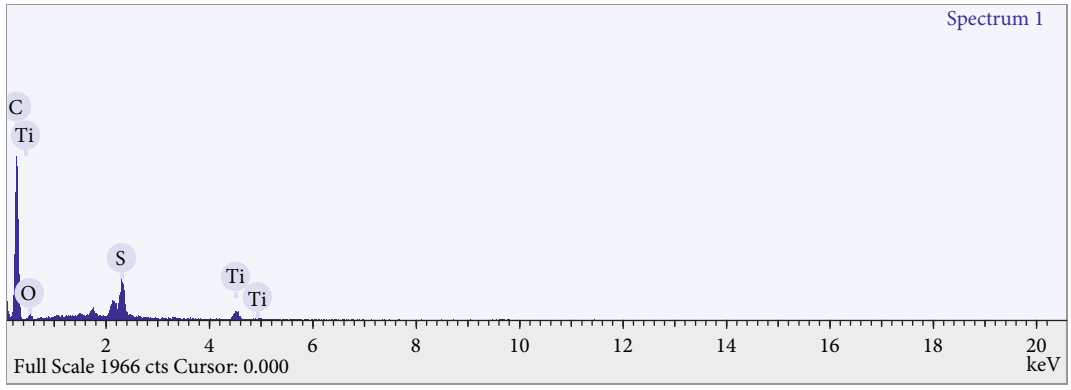

Quantification Settings

Quantification method : All elements (normalised) Coating element : None

Summary results

Element	Weight %	Weight % σ	Atomic %
Carbon	84.938	1.218	91.884
Oxygen	6.221	1.270	5.053
Sulfur	4.962	0.274	2.011
Titanium	3.879	0.277	1.052

(f)

Figure 7: (a) Control Sample. (b) 1% nano TiO_2 modified bitumen. (c) 2% nano TiO_2 modified bitumen. (d) 3% nano TiO_2 modified bitumen. (e) 4% nano TiO_2 modified bitumen. (f) 5% nano TiO_2 modified bitumen.

permanent deformation in SMA [22]. Figure 11 shows the stability and flow for various nano titanium percentages. 0% nano TiO_2 yields the highest flow, although further nano TiO_2 addition reduces the flow value.

3.6.2. Flow. Figures 12 and 13 show the flow performance of asphalt mixtures with different nano TiO_2 percentages. The flow value indicates the flexibility of asphalt mixtures [23]. The modified SMA20 mixture produces an inconsistent flow value

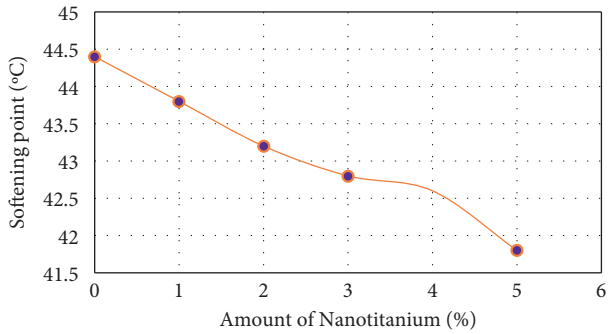

Figure 8: The softening point of nano TiO_2 modified bitumen.

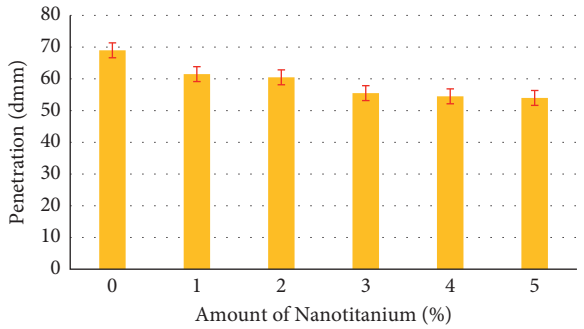

Figure 9: Penetration values of nano TiO_2 modified binder.

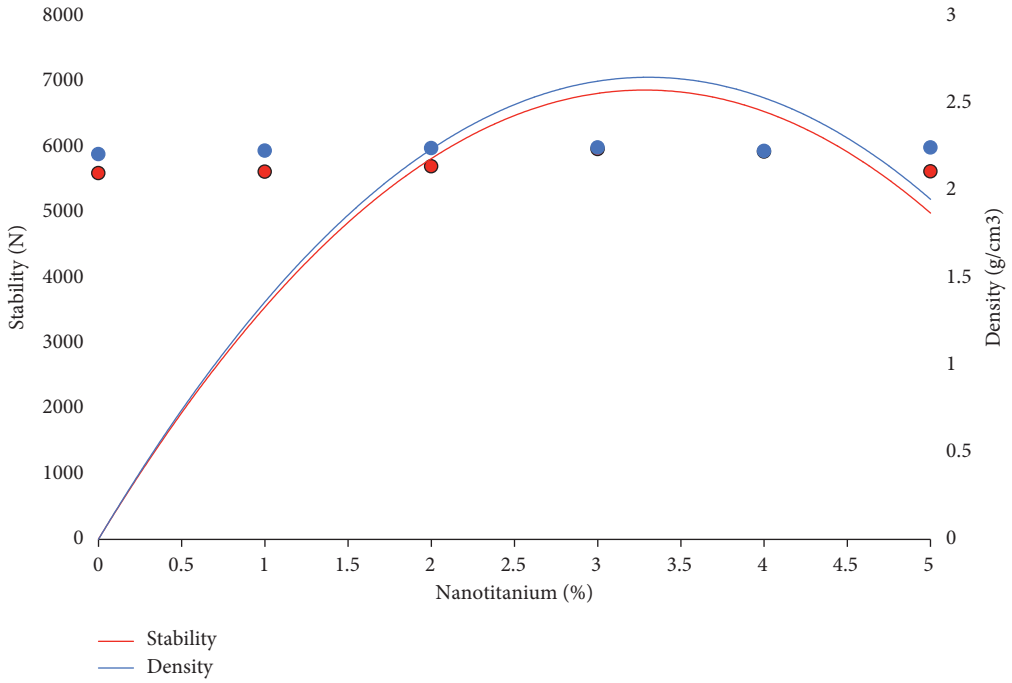

Figure 10: Stability and density against nano TiO_2 percentages.

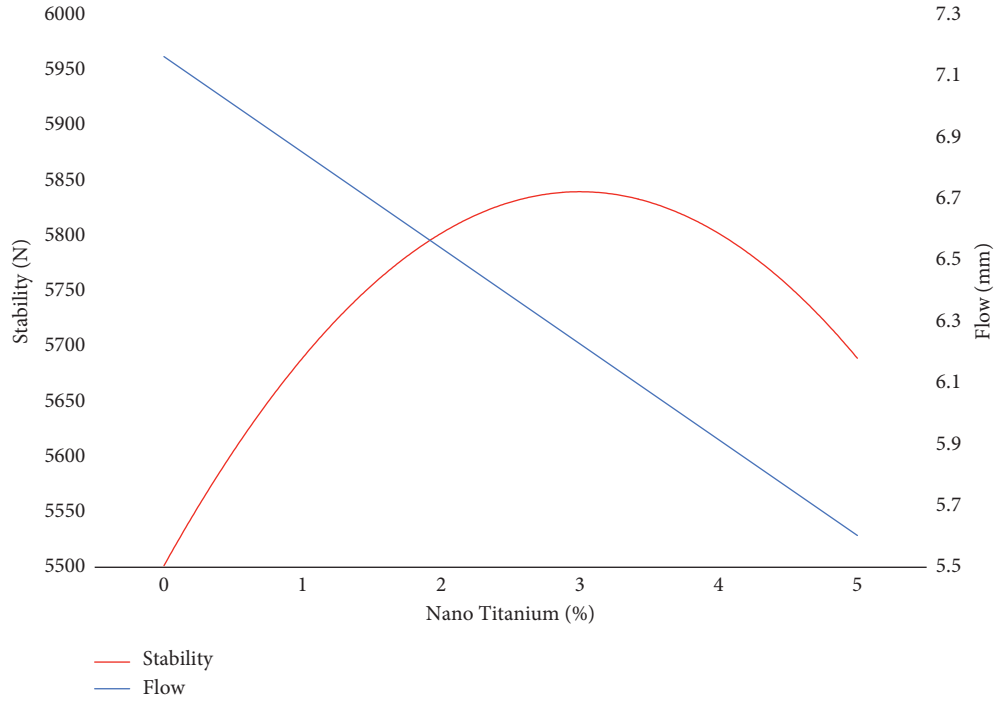

Figure 11: Stability and flow against nano TiO_2 percentages.

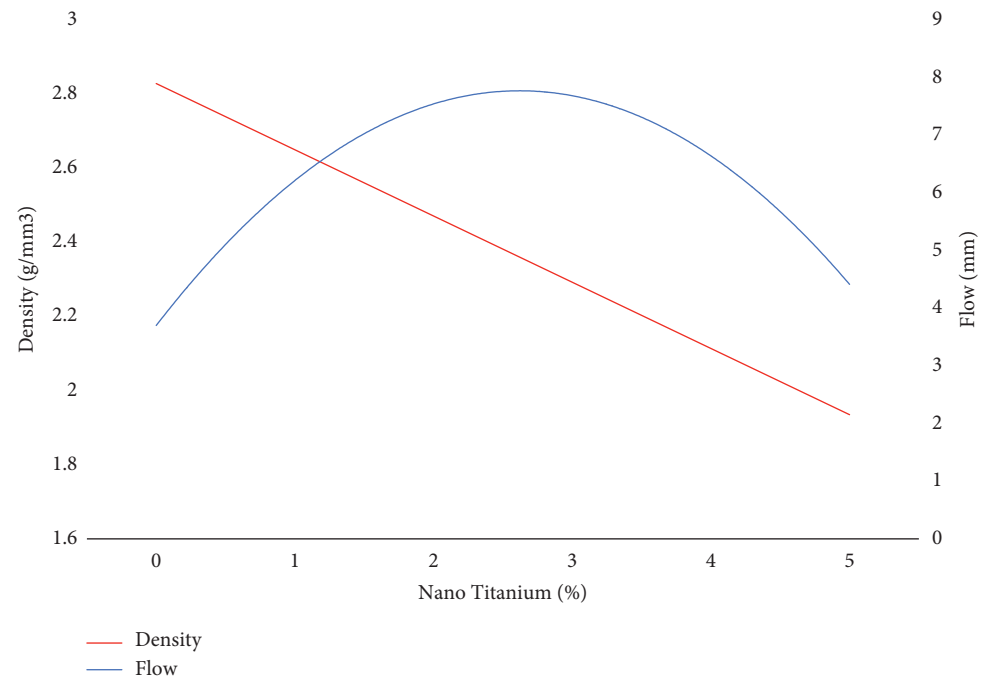

Figure 12: Density and flow against nano TiO_2 percentage.

with the inclusion of nano TiO_2. The flow at 3% nano TiO_2 complements both the density and stiffness. 0% nano TiO_2 produces a relatively higher flow value (7 mm) than the requirement by the Public Work Department (between 3 to 5 mm). The addition of nano TiO_2 reduces the flow, indicating that nano TiO_2 could influence the flow properties to a more accustomed value.

3.6.3. Stiffness. Figures 14 and 15 exhibits the stiffness of SMA mixtures against various nano TiO_2 percentages. The highest stiffness value is obtained by the 3% nano TiO_2 addition (965.67 N/mm), compared to 833.3 N/mm for 0% nano TiO_2 which is a 14.8% improvement. This shows that nano TiO_2 addition improves the stiffness characteristic of asphalt mixture.

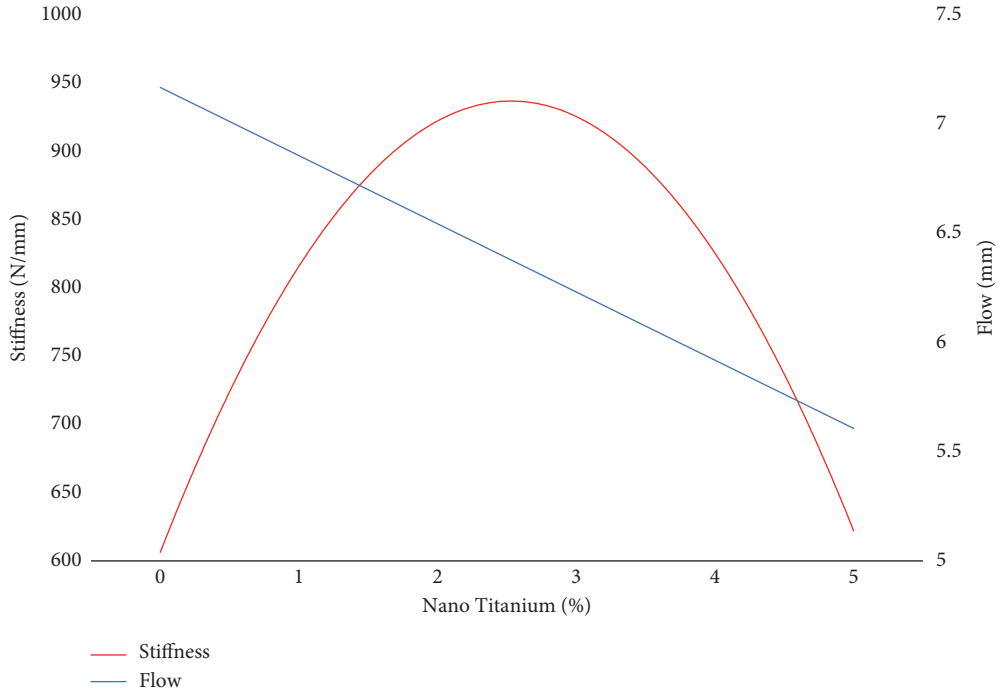

Figure 13: Stiffness and flow against nano TiO_2 percentages.

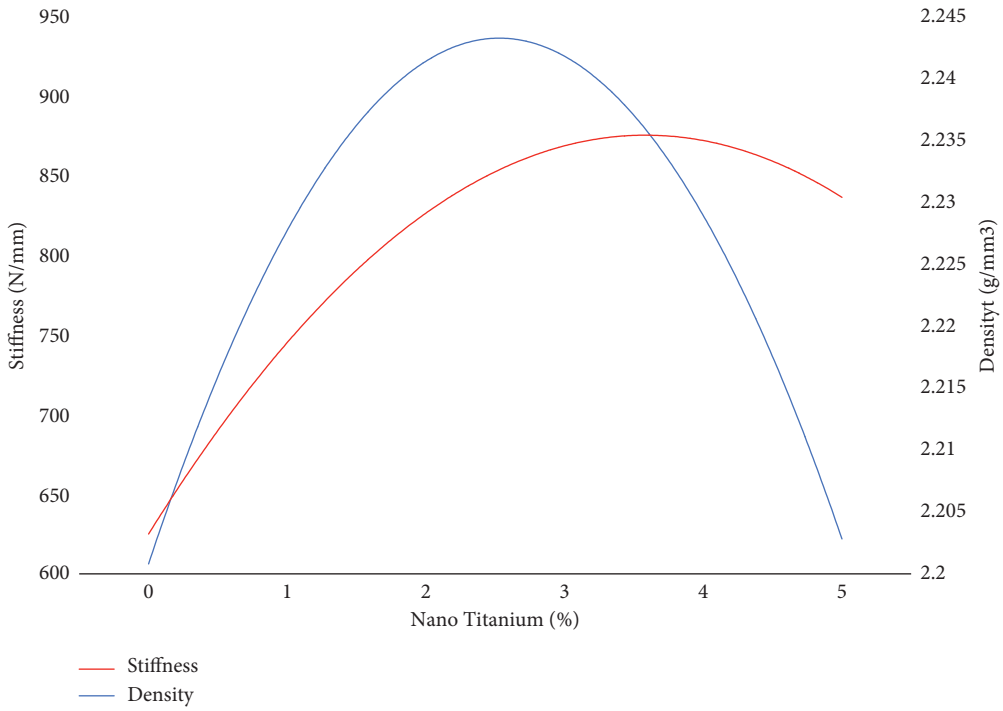

Figure 14: Stiffness and density against nano TiO_2 percentages.

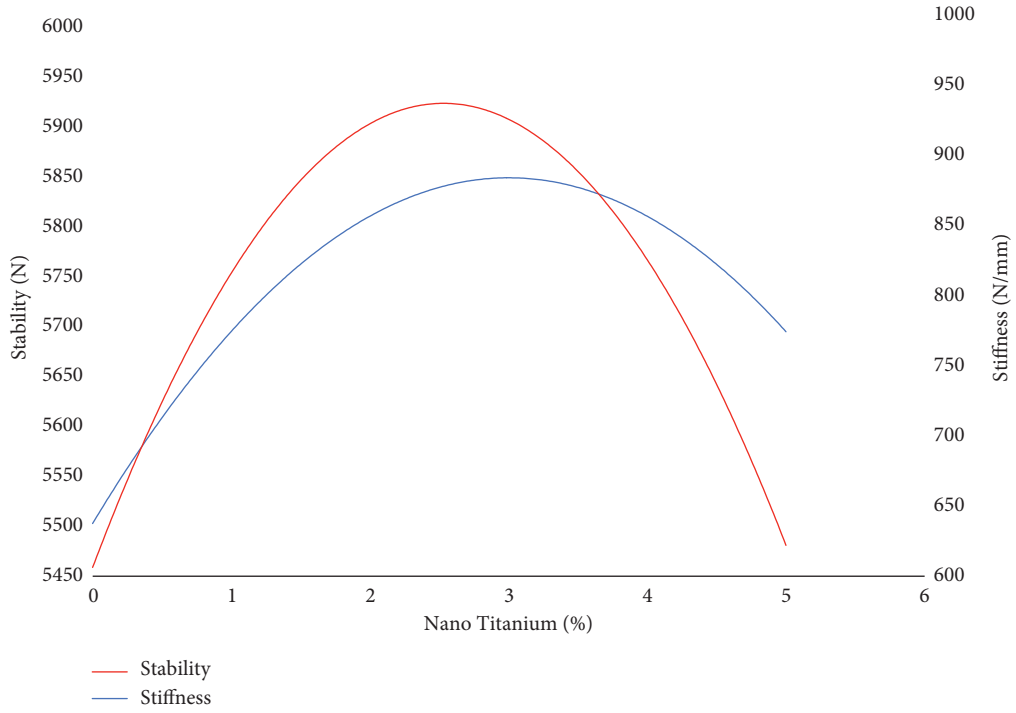

Figure 15: Stability and stiffness against nano TiO_2 percentages.

4. Conclusion

The nano TiO_2 modified binder significantly improves the microstructural, chemical, and physical properties of bitumen, as well as enhancing the mechanical properties of the SMA mixture. The details are as follows:

(a) From FTIR results, the change in chemical bonds happens when the nano TiO_2 is added into the bitumen showing that the nano TiO_2 successfully blends into the bitumen.

(b) XRD analysis peaks are higher and further compared to the virgin bitumen which has lower peak starting. This proved the existence of nano TiO_2 in the virgin bitumen.

(c) SEM-EDX results show that bitumen mixture particles are well dispersed depending on the nano TiO_2 percentages. The 3% addition of nano TiO_2 reveals that it is able to merge the nano TiO_2 particles fully into the bitumen.

(d) The penetration and softening point show a consistent trend similar to previous research studies as discussed earlier showing that 3% to 5% nano modification contributes the optimum value.

(e) Improvements of the physical, morphological, and chemical characteristics also enhance the mechanical performance of SMA as evident from volumetric properties.

The density, stability, flow, and stiffness properties of the 3% nano TiO_2 addition mixture are better than the 0% nano TiO_2 due to the addition of the modified nano TiO_2 binder. Therefore, it can be concluded that overall, 3% nano TiO_2 addition enhances the mechanical properties of SMA. Finally, the improvement of nano TiO_2 modified binder directly enhances the quality of SMA performance in terms of its volumetric properties [22].

Data Availability

All the data used to support the findings of this study are included within the article.

Conflicts of Interest

The authors declare that they have no conflicts of interest with other entities or researchers.

Acknowledgments

The authors would like to express gratitude to Universiti Malaysia Pahang and the Ministry of Higher Education to fund this research. This research was funded by Universiti Malaysia Pahang, under grant RDU1903146 and RDU190387. The RUI grant (1001.PAWAM.8014140) and Incentive grant from Universiti Sains Malaysia are also highly appreciated.

References

[1] A. Ameli, J. Maher, A. Mosavi, N. Nabipour, R. Babagoli, and N. Norouzi, "Performance evaluation of binders and stone matrix asphalt (SMA) mixtures modified by ground tire rubber (GTR), waste polyethylene terephthalate (PET) and anti stripping agents (ASAs)," *Construction and Building Materials*, vol. 251, Article ID 118932, 2020.

[2] S. Eskandarsefat, G. Dondi, and C. Sangiorgi, "Recycled and rubberized SMA modified mixtures: A comparison between polymer modified bitumen and modified fibres," *Construction and Building Materials*, vol. 202, pp. 681–691, 2019.

[3] N. E. Jasni, K. A. Masri, P. J. Ramadhansyah et al., "Mechanical performance of stone mastic asphalt incorporating steel fiber," *IOP Conference Series: Materials Science and Engineering*, vol. 712, no. 1, Article ID 012026, 2020.

[4] J. Choudhary, B. Kumar, and A. Gupta, "Utilization of solid waste materials as alternative fillers in asphalt mixes: A review," *Construction and Building Materials*, vol. 234, Article ID 117271, 2020.

[5] P. Caputo, M. Porto, R. Angelico, V. Loise, P. Calandra, and C. O. Rossi, "Bitumen and asphalt concrete modified by nanometer-sized particles: Basic concepts, the state of the art and future perspectives of the nanoscale approach," *Advances in Colloid and Interface Science*, vol. 285, Article ID 102283, 2020.

[6] S. A. Mazari, E. Ali, R. Abro et al., "Nanomaterials: applications, waste-handling, environmental toxicities, and future challenges - A review," *Journal of Environmental Chemical Engineering*, vol. 9, no. 2, 2021.

[7] M. Motamedi, G. Shafabakhsh, and M. Azadi, "Evaluation of fatigue and rutting properties of asphalt binder and mastic modified by synthesized polyurethane," *Journal of Traffic and Transportation Engineering (English Edition)*, vol. 8, no. 6, pp. 1036–1048, 2021.

[8] H. Hong, H. Zhang, and S. Zhang, "Effect of multi-dimensional nanomaterials on the aging behavior of asphalt by atomic force microscope," *Construction and Building Materials*, vol. 260, Article ID 120389, 2020.

[9] Y. He, Z. Wang, H. Wang et al., "Metal-organic framework-derived nanomaterials in environment related fields: Fundamentals, properties and applications," *Coordination Chemistry Reviews*, vol. 429, Article ID 213618, 2021.

[10] P. J. Ramadhansyah, K. A. Masri, A. H. Norhidayah et al., "Nanoparticle in asphalt binder: A state-of-the-art review," *IOP Conference Series: Materials Science and Engineering*, vol. 712, no. 1, Article ID 012023, 2020.

[11] K. Snehal, B. B. Das, and M. Akanksha, "Early age , hydration , mechanical and microstructure properties of nano-silica blended cementitious composites," *Construction and Building Materials*, vol. 233, Article ID 117212, 2020.

[12] C. N. Fernandes, R. L. S. Ferreira, R. D. S. Bernardo, F. Avelino, and A. A. Bertini, "Using TiO2 nanoparticles as a SO2 catalyst in cement mortars," *Construction and Building Materials*, vol. 257, pp. 2–10, 2020.

[13] L. Zhang, Q. Lu, R. Shan, F. Zhang, Y. Muhammad, and K. Huang, "Photocatalytic degradation of vehicular exhaust by nitrogen-doped titanium dioxide modified pavement material," *Transportation Research Part D: Transport and Environment*, vol. 91, Article ID 102690, 2021.

[14] A. Ameli, A. H. Pakshir, R. Babagoli, N. Norouzi, D. Nasr, and S. Davoudinezhad, "Experimental investigation of the influence of Nano TiO2 on rheological properties of binders and performance of stone matrix asphalt mixtures containing steel slag aggregate," *Construction and Building Materials*, vol. 265, Article ID 120750, 2020.

[15] R. Babagoli, "Laboratory investigation of the performance of binders and asphalt mixtures modified by carbon nano tube, poly phosphoric acid, and styrene butadiene rubber," *Construction and Building Materials*, vol. 275, Article ID 122178, 2021.

[16] A. K. Arshad, J. Ahmad, and K. A. Masri, "Rutting resistance of nanosilica modified porous asphalt," *International Journal of Civil Engineering & Technology*, vol. 10, no. 1, pp. 2274–2284, 2019.

[17] P. Lin, C. Yan, W. Huang et al., "Rheological, chemical and aging characteristics of high content polymer modified asphalt," *Construction and Building Materials*, vol. 207, pp. 616–629, 2019.

[18] S. H. Razavi and A. Kavussi, "The role of nanomaterials in reducing moisture damage of asphalt mixes," *Construction and Building Materials*, vol. 239, Article ID 117827, 2020.

[19] A. K. Arshad, M. S. Samsudin, J. Ahmad, and K. A. Masri, "Microstructure of nanosilica modified binder by atomic force microscopy," *Jurnal Teknologi*, vol. 78, no. 7-3, 2016.

[20] J. M. L. Crucho, J. M. C. D. Neves, S. D. Capitão, and L. G. D. P. Santos, "Mechanical performance of asphalt concrete modified with nanoparticles: Nanosilica, zero-valent iron and nanoclay," *Construction and Building Materials*, vol. 181, pp. 309–318, 2018.

[21] N. A. N. M. Fauzi, K. A. Masri, P. J. Ramadhansyah et al., "Volumetric properties and resilient modulus of stone mastic asphalt incorporating cellulose fiber," *IOP Conference Series: Materials Science and Engineering*, vol. 712, Article ID 012028, 2020.

[22] P. J. Ramadhansyah, K. A. Masri, H. Awang et al., "Stability and stiffness of asphaltic concrete incorporating waste cooking oil," *International Journal of Recent Technology and Engineering*, vol. 7, no. 6, pp. 2277–3878, 2019.

[23] M. Ahmad, S. Beddu, S. Hussain, A. Manan, and Z. B. Itam, "Mechanical properties of hot-mix asphalt using waste crumber rubber and phenol formaldehyde polymer," *AIMS Materials Science*, vol. 6, no. 6, pp. 1164–1175, 2019.